JCEC
THE JOURNAL OF ENGINEERING AND EXACT SCIENCES

OPEN ACCESS

The Journal of Engineering and Exact Sciences – jCEC, Vol. 09 N. 05 (2023)
journal homepage: https://periodicos.ufv.br/jcec
eISSN: 2527-1075
ISSN: 2446-9416

Parametric Study of Rider's Comfort in a Vehicle with Semi-Active Suspension System Under Steady State Conditions

Article Info:
Article history: Received 2022-12-22 / Accepted 2023-02-10 / Available online 2023-02-10
doi: 10.18540/jcecvl9iss5pp15377-01e

Arinola Bola Ajayi
ORCID: https://orcid.org/0000-0002-4733-0803
Department of Mechanical Engineering, University of Lagos, Lagos, Nigeria
E-mail: abajayi@unilag.edu.ng
Sunday Joshua Ojolo
ORCID: https://orcid.org/0000-0002-4548-0090
Department of Mechanical Engineering, University of Lagos, Lagos, Nigeria
E-mail: sojolo@unilag.edu.ng
Ediketin Ojogho
ORCID: https://orcid.org/0000000155662683
Department of Aerospace Engineering, Lagos State University, Ojo, Lagos, Nigeria
E-mail: ediketin96@gmail.com
Antonio Marcos de Oliveira Siqueira
ORCID: https://orcid.org/0000-0001-9334-0394
Federal University of Viçosa, Brazil
E-mail: antonio.siqueira@ufv.br

Abstract

Due to the influence of road roughness on all quantities representing dynamic response of vehicles such as vehicle ride comfort, tire dynamic force, dampers and spring forces, etc., the interaction between a vehicle and road profiles in relation to the comfort and health of passengers has become significant as road roughness causes a spectrum of oscillations for a moving vehicle. Thus, this study investigates the dynamic response of semi-active vehicle suspension system under the influence of steady state road conditions such as smooth, gravel and suburban roads to obtain mathematical equations based on the pitch and heave motions of the vehicle. Power spectral density, PSD, was used to characterize the road input spectrum on the basis of the road roughness parameters which correlate with International Roughness Index, (IRI). Vehicle suspension system responses to the different road inputs were obtained by simulation based on the mathematical model developed using Matlab/Simulink software. The root-mean-square acceleration was used as objective metric to estimate the passenger's discomfort, dynamic tire force and suspension travel at a constant vehicle speed of 20 km/h while the ISO 2631 was applied to predict the discomfort experienced by the riders under different steady state road irregularities. The discomfort experienced by the riders on the gravel road and suburban road increased when the vehicle parameters were increased and also when the speed of the vehicle was increased. For smooth road, the riders experienced comfort according to ISO 2631, although the discomfort threshold increased with increase in speed of the vehicle but still within the threshold of human comfort zone. It can be concluded that for a vehicle ride within the human comfort zone on gravel and suburban roads, the speed of the vehicle should be brought down considerable below 20 km/h and the suspension systems should also be improved upon.

Keywords: Vehicle ride comfort. Steady state road conditions. Dynamic tire force. Power spectral density. Road roughness index.

Nomenclature

$a_1,\ a_2,\ a_3$	distances between the front and rear suspensions and the vehicle body from center of center of gravity
c_2, c_3	lower and upper limb damper
$C_{sf}\ , C_{sr}$	Front and rear suspension damper of sprung mass
C_{uf}, C_{ur}	Front and rear suspension damper of unsprung mass
F_{df}, F_{dr}	Damping forces of the front and rear half-car suspension model
$F_{sf},\ F_{sr}, F_{uf}, F_{ur}$	Upward force on the system due to front suspension and rear suspension of sprung and unsprung masses
$F_{u,}F_z$	Force function of front and rear control and force function of road input
$h_0,$	Height of road bump
G	Center of gravity
J	Polar Moment of inertia
k_2, k_3	Spring constant of the lower and upper limb
$k_{se},\ c_{se}$	Spring and damper of seat
$K_{sf}\ \ K_{sr}$	Front and rear suspension stiffness of sprung mass
$K_{uf}\ ,\ K_{ur}$	Front and rear suspension stiffness of unsprung mass
m_b	Vehicle body mass
m_{se}, m_2, m_3	Masses of seat, lower limb and upper limb
M_{Sf}, M_{sr}	Sprung masses of front and rear suspensions
M_{uf}, M_{ur}	Unsprung masses of front and rear suspensions
$q_b,\ \dot{q}_b$	Vertical displacement and velocity of seat
$u_f\ , u_r$	Control forces of the front and rear suspension
$v_0,$	Velocity of vehicle
w_b	Width of road bump
x_b	The vertical displacement of sprung mass about the center of gravity
x_{se}, x_2, x_3	Displacement of seat, lower and upper limb
$\dot{x}_{se}, \dot{x}_2, \dot{x}_3$	Velocities of the seat, lower and upper limb
$\ddot{x}_{se}, \ddot{x}_2, \ddot{x}_3$	Accelerations of the seat, lower and upper limb
x_{sf}, x_{sr}	Vertical displacement of front and rear sprung mass about the center of gravity
$x_{uf}\ x_{ur},$	Vertical displacement of the front and rear unsprung mass
$z_f(t),\ z_r(t)$	Sinusoidal road induced disturbance to the front and rear wheels
$z, \dot{z}$	Displacement and velocity of the road input function
$z_f,\ z_r$	Disturbances at the front and the rear due to the movement of the vehicle over an uneven road disturbances
$\dot{z}_{f,}\ \dot{z}_r$	Velocities of the front and rear due to road input
ω	Natural frequency of road distribution
$\theta,\ \dot{\theta},\ \ddot{\theta}$	Angular displacement Pitch rate of change and Angular acceleration of the body

1. Introduction

When a vehicle traverses road irregularities, the disturbance from the road influences its ride performance characteristics and handling stability (Gohrle et al. 2014; Kim and Choi, 2016). Consequently, the suspension system is an important component that plays a critical function in the transmission of force between vehicle tire and body of the vehicle, and reduces the impact of the road on the riders. Vehicle suspension system is the term used to describe systems of springs, shock absorbers or dampers and linkages that connects a vehicle to its wheels. Shock absorbers are important parts of the vehicle suspension system which have effects on the ride performance characteristics of the vehicle. They are also critical for tire to road contact to reduce the tendency of a tire to lift off the road. They affect braking, steering, cornering and overall stability of the vehicle. Absences of shock absorbers from vehicle suspension system may cause vehicle to bounce up and down continuously. Although most passenger vehicle suspension systems provide acceptable ride on smooth road surfaces, some performed badly when traversing rough terrain such as gravel roads, and suburban roads.

The ride performance characteristics of a vehicle suspension under steady state conditions that is smooth roads, gravel roads and suburban roads may be expressed in terms of the suspension travel and dynamic tire force to evaluate the discomfort felt by the rider. The root-mean-square (rms) acceleration serves as objective metric to evaluate the performance of the vehicle due to input from different steady state road conditions (Sharp and Hassan, 1986; Thompson, 1989; Abdel Hady, 1989). Thus, the root-mean-square acceleration is a measure of the vibration power absorbed by vehicle rider. Attempts have been made to correlate subjective assessment of vehicle ride discomfort with objective measurement of body acceleration by applying various weighting functions (Griffin, 1990). Using the results of a large number of experiments, the International Standard Organization, ISO produced weighting functions for equalizing the discomfort produced by vibration at different frequencies (ISO 2631, 1997).

The disturbance from the road roughness can be analyzed by using the power spectral density, PSD. By using the road roughness parameters which correlate with the International Roughness Index, the power spectral density, PSD, has been adopted to characterize the road input spectrum. Using this technique, Mitchell and Gyenes (1989) used dynamic pavement load to measure the velocity of truck suspension due to the road roughness while Stoica and Moses (1997) used the method to translate the time domain data into the frequency domain to show how the power of signal or time series is distributed over frequency. Using the results from the International Road Roughness Experiment performed in Brazil in 1982, Sayers and Karamihas (1997) characterized different road roughness. Since then, it has become a well-recognized standard for the measurement of road roughness. The random road unevenness of longitudinal road profile which is the source of excitation of a moving vehicle was provided on the basis of road profile waviness by Decky and Valuch (2000). Thus, the power spectral density, PSD provides information about the characterization of road profiles using road roughness values from IRI and selected waviness (Davis and Thompson, 2001). Many **r**oad profile simulations are carried out using specialized software packages which generate road profile signals on a user-defined power spectral density, PSD. In literature, various procedures had been presented to generate random time domain signal with given spectral density using periodic functions (Rouillard, et al 2001). The road profiles are simulated by a program written in Matlab environment based on selected PSD parameters (Stoica and Moses, 1997; Sayer and Karamihasi, 1997; Sun, 2002).

This research focuses on predicting discomfort experienced by riders based on vehicle responses formulated by modeling a 4 degree-of–freedom half car model integrated with 3 degrees of freedom sub-human seat arrangement. The dynamic properties of the semi-active vehicle suspension systems are contrived on the basis of linear mass-spring damper characteristics and the rider's discomfort were evaluated.

2.0 Methodology

2.1 Model Description

This study is based on 7 degree of freedom vehicle model (Ajayi, et al. 2023) which is a combination of a 4 degree of freedom half car semi-active vehicle model and a 3 degree of freedom subhuman-seat arrangement as shown in Fig. 1. The spring-damper characteristics are modeled as simple linear system with passive elements of translational nature, being concentrically placed between the car body and the axle.

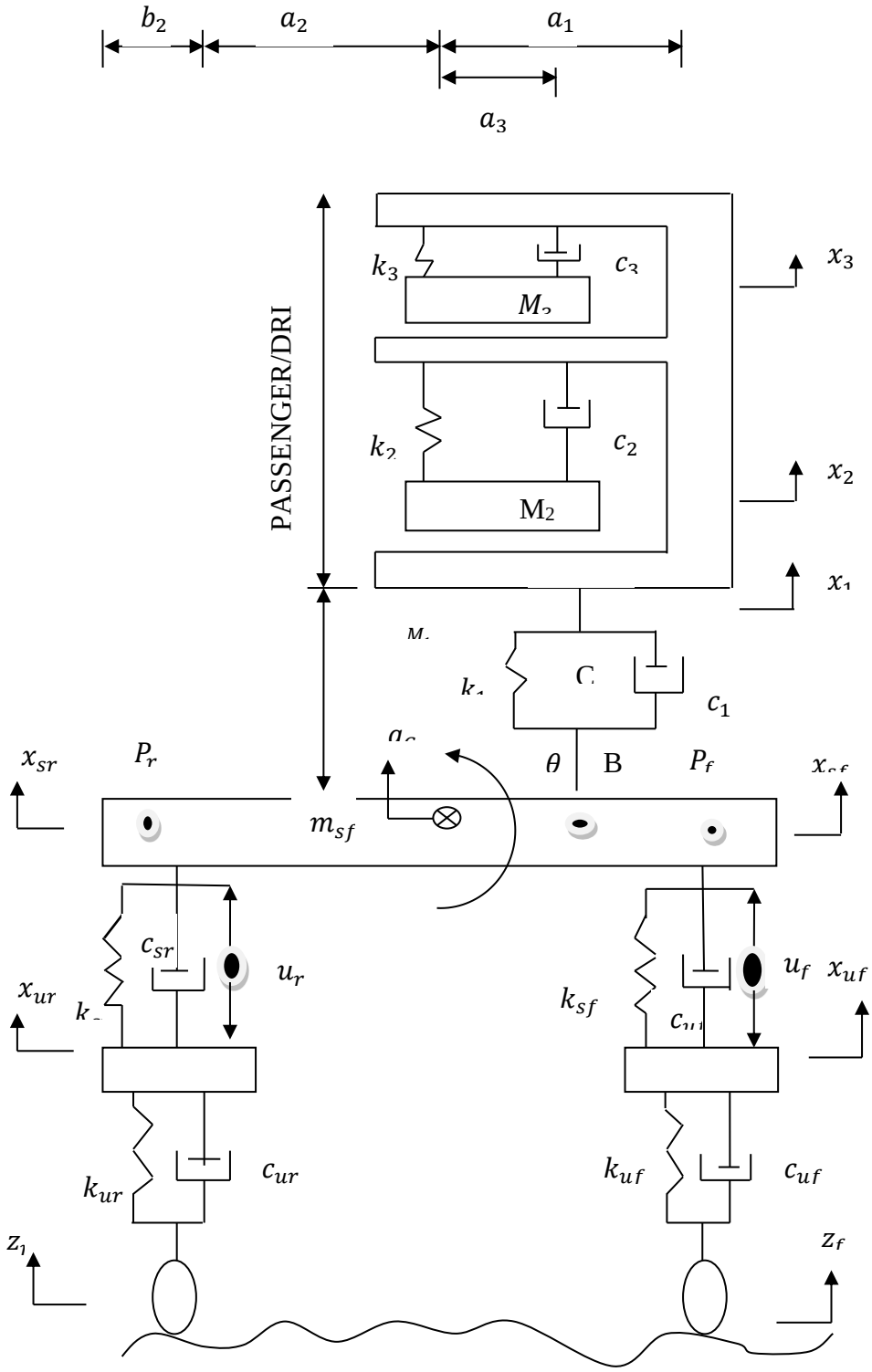

Figure 1: Half-car vehicle model with human-seat (Ajayi, et. al, 2023)

The half-car model takes into account both translational and rotational motions of the sprung mass. It assumes the symmetry of the car about the longitudinal axis as well as equal suspension characteristics for both front wheels and likewise for both rear wheels. The half car model makes the following assumptions: The contact with the road is a point contact. This is a simple model of the tire. Linear springs and dampers were also assumed when simulating a vehicle. As the suspension only produces stiffness in the vertical direction, only vertical displacement is considered.

A seat-human subsystem is included in the semi-active vehicle suspension system in order to assess the performance of the model in relation to the ride comfort of the passengers. To represent the human body joint, kinematic constraints and spring-damper elements are used to connect each part. The human body is composed of the lower and upper bodies. The lower body includes the legs and thigh (pelvic) while the upper body includes the arm and chest parts of the human body. The lower and upper body segments are represented as biomechanical system with springs and damper characteristics.

The sub-human body interacts with the suspension by means of the vehicle seat. The vehicle seat is modeled by mass, m_{se}, the spring, k_{se} and damper, c_{se} while the human system is composed of masses m_2 and m_3; springs k_2 and k_3, dampers c_2 and c_3. The point C represents the driver or passenger position and point B, located at a distance a_3 from the center of gravity of the vehicle body is the distance between vehicle body and the seat–driver subsystem.

2.2 Mathematical Model

The seven degrees of freedom resulting from half-car and seat suspension model are governed by the equations fully developed by Ajayi, et al (2023) and given in matrix form in equation (1);

$$[M]\{\ddot{x}\} + [C]\{\dot{x}\} + [K]\{x\} = \{F\} \tag{1}$$

where

$$[M] = \begin{bmatrix} m_3 & 0 & 0 & 0 & 0 & 0 & 0 \\ 0 & m_2 & 0 & 0 & 0 & 0 & 0 \\ 0 & 0 & m_{se} & 0 & 0 & 0 & 0 \\ 0 & 0 & 0 & m_b & 0 & 0 & 0 \\ 0 & 0 & 0 & 0 & m_{uf} & 0 & 0 \\ 0 & 0 & 0 & 0 & 0 & m_{ur} & 0 \\ 0 & 0 & 0 & 0 & 0 & 0 & J \end{bmatrix}$$

$$[C] = \begin{bmatrix} c_3 & 0 & -c_{se} & 0 & 0 & 0 & 0 \\ 0 & c_2 & -c_{se} & 0 & 0 & 0 & 0 \\ -c_3 & -c_2 & c_{se}+c_2+c_3 & -c_{se} & 0 & 0 & c_{se}a_3 \\ 0 & 0 & C_{se} & c_{sf}+c_{sr}+c_{se} & -c_{sf} & -c_{sr} & c_{sr}a_2 - c_{sf}a_1 - c_{se}a_3 \\ 0 & 0 & 0 & -c_{sf} & c_{uf}+c_{sf} & 0 & c_{sf}a_1 \\ 0 & 0 & 0 & -c_{sr} & 0 & c_{ur}+c_{sr} & -c_{sr}a_2 \\ 0 & 0 & c_{se}a_3 & c_{sf}a_1 - c_{sr}a_2 + c_{se}a_3 & -c_{sf}a_1 & c_{sr}a_2 & -\left(c_{sr}a_2^{\,2} + c_{sf}a_1^{\,2} + c_{se}a_3^{\,2}\right) \end{bmatrix}$$

$$[K]=\begin{bmatrix} k_3 & 0 & -k_3 & 0 & 0 & 0 & 0 \\ 0 & k_2 & -k_2 & 0 & 0 & 0 & 0 \\ -k_3 & -k_2 & k_{se}+k_2+k_3 & k_{se} & 0 & 0 & k_{se}a_3 \\ 0 & 0 & -k_{se} & k_{sf}+k_{sr}+k_{se} & -k_{sf} & -k_{ur} & k_{sr}a_2-k_{sf}a_1-k_{se}a_3 \\ 0 & 0 & 0 & -k_{sf} & k_{uf}+k_{sf} & 0 & k_{sf}a_1 \\ 0 & 0 & 0 & -k_{sr} & 0 & k_{sr}+k_{ur} & k_{sr}a_2 \\ 0 & 0 & k_{se}a_3 & k_{sr}a_2-k_{sf}a_1+k_{se}a_3 & k_{sf}a_1 & -k_{sr}a_2 & k_{sf}a_1^2+k_{sr}a_2^2+k_{se}a_3^2 \end{bmatrix}$$

$$[F_u]=\begin{Bmatrix} 0 \\ 0 \\ 0 \\ u_f+u_r \\ -u_f \\ -u_r \\ a_1u_f-a_2u_r \end{Bmatrix} \text{ and } [\boldsymbol{F_z}] = \begin{Bmatrix} 0 \\ 0 \\ 0 \\ 0 \\ k_{uf}z_f+c_{uf}\dot{z}_f \\ k_{ur}z_r+c_{ur}\dot{z}_r \\ 0 \end{Bmatrix} = \begin{Bmatrix} 0 \\ 0 \\ 0 \\ 0 \\ (k_{uf}+j\omega c_{uf})z_f \\ (k_{ur}+j\omega c_{ur})z_r \\ 0 \end{Bmatrix}$$

$\dot{z}_f = j\omega z_f, \quad \dot{z}_r = j\omega z_r$ are time derivative of z_f *and* z_r respectively
$[M]$, $[C]$ and $[K]$ are mass, damping and stiffness matrices respectively;
$\{X\}$, $\{\dot{x}\}$ and $\{\ddot{x}\}$ are the displacement, velocity and acceleration vectors respectively;
$[F_u]$ and $[\mathrm{F_z}]$ are the force functions.

The vectors $\{z_f\}, \{\dot{z}_f\}, \{z_r\}, \{\dot{z}_r\}$ are displacements and velocities of front and rear tires due to road input.

Based on the passenger vehicle model for the study, displacement vector, velocity vector and acceleration vector matrices are formulated. For example, displacements of the upper body, x_3 of passenger comes before that of the lower body, x_2 etc.

$$\{x\} = \begin{Bmatrix} x_3 \\ x_2 \\ x_{se} \\ x_b \\ x_{uf} \\ x_{ur} \\ \theta \end{Bmatrix} \{\dot{x}\} = \begin{Bmatrix} \dot{x}_3 \\ \dot{x}_2 \\ \dot{x}_{se} \\ \dot{x}_b \\ \dot{x}_{uf} \\ \dot{x}_{ur} \\ \dot{\theta} \end{Bmatrix} \{\ddot{x}\} = \begin{Bmatrix} \ddot{x}_3 \\ \ddot{x}_2 \\ \ddot{x}_{se} \\ \ddot{x}_b \\ \ddot{x}_{uf} \\ \ddot{x}_{ur} \\ \ddot{\theta} \end{Bmatrix} \quad (2)$$

2.3 Vehicle Suspension Parameters with Human and Seat Arrangement

Appropriate parameter selection in vehicle suspension system characterization is aimed at providing an isolation of vehicle body from road irregularities and to ensure good road holding and riders' comfort. The parameters used are derived from mid-sized saloon car shown in Table 1 and human biomechanical system given in Table 2. This is significant because of the widespread use of the vehicle types for passengers, lower cost of purchase, effects of vibration on the vehicle occupants and the ride performance characteristics of the vehicles as they traversed the road conditions.

Table 1: Suspension parameters used (Raji, 2013)

Parameter	Symbol	Values	Unit
Sprung mass of vehicle chassis	m_b	575	Kg
Moment of inertia of the vehicle	J	769	Kgm^2
Unsprung mass of the front axle	m_{uf}	60	Kg
Unsprung mass of the rear axle	m_{ur}	60	Kg
Stiffness of the front tire	k_{uf}	190	kN/m
Stiffness of the rear tire	k_{ur}	190	kN/m
Damping coefficient of front tyre	c_{uf}	350	Ns/m
Damping coefficient of rear tyre	c_{ur}	350	Ns/m
Stiffness of the front axle	k_{sf}	16812	N/m
Stiffness of the rear axle	k_{sr}	16812	N/m
Damping coefficient of the front axle	c_{sf}	1000	Ns/m
Damping coefficient of the rear axle	c_{sr}	1000	Ns/m
Front body length from CG	a_1	1.4	m
Rear body length from CG	a_2	1.4	m
Seat-driver distance from CG	a_3	0.65	m

Table 2: Biomechanical parameters of the human system (Abbas et al, 2010)

Parameter	Symbol	Values	Unit
Mass of lower limb	m_2	5.5	Kg
Mass of upper limb	m_3	36	Kg
Stiffness of lower limb	k_2	144000	N/m
Stiffness of upper limb	k_3	20000	N/m
Damping coefficient of lower limb	c_2	909	Ns/m
Damping coefficient of upper limb	c_3	330	Ns/m

2.4 Steady State Road Conditions

Steady state ride occurs when the vehicle is travelling at a constant velocity on a straight road. This is characterized by the power spectral densities, PSDs. It is expressed in equation (3) (Stoica and Moses, 1997; Sayer and Karamihasi, 1997; Sun, 2002) as

$$PSD = \frac{C_r}{v^{\alpha}} m^3/cycle \tag{3}$$

Where
C_r = road roughness index
α = wavenumber (frequency characteristics of the road)

Converting equation (3) to function of road speed and frequency domain, the power spectral density, PSD function is expressed in equation (4) as

$$PSD = \left(\frac{U}{f}\right)^{\alpha} \frac{1}{U} = C_r \frac{U^{\alpha-1}}{f^{\alpha}} \tag{4}$$

where
U = vehicle speed (km/h),
f = frequency (Hz)

2.5 Road Roughness Profile for Steady State Conditions:

Table 3 shows the road roughness characteristics for smooth, gravel and suburban roads used in this study. Only the road profile simulations for gravel road with road surface roughness index, Cr = 4.4 x 10^{-6}, α = 2.1 and vehicle speed of 20km/h using the power spectral density, PSD characterization are considered and shown in Fig. 3 and 4

Table 3: Road Roughness Characteristics

Nature of road	Characteristics	Wavenumber	Roughness Index
Highway	Smooth highway	2.1	4.8×10^{-7}
Pavement	Highway with gravel	2.1	4.4×10^{-6}
Rough runway (suburban)	Poorly kept rough road	2.1	8.1×10^{-6}

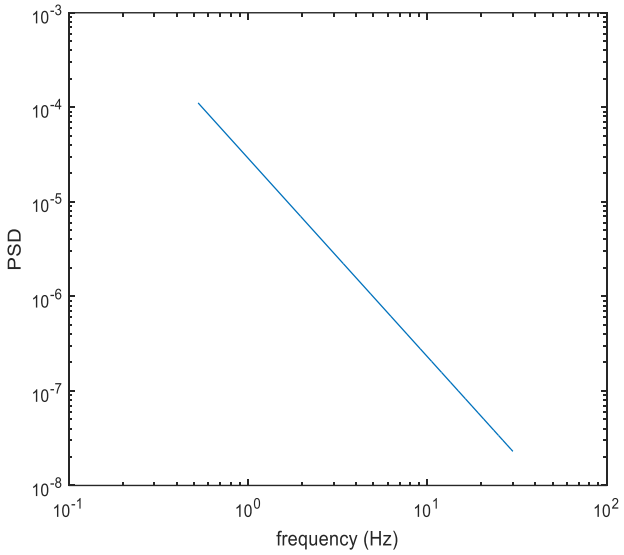

Figure 3: Power Spectral Density against Frequency at 20km/h vehicle speed

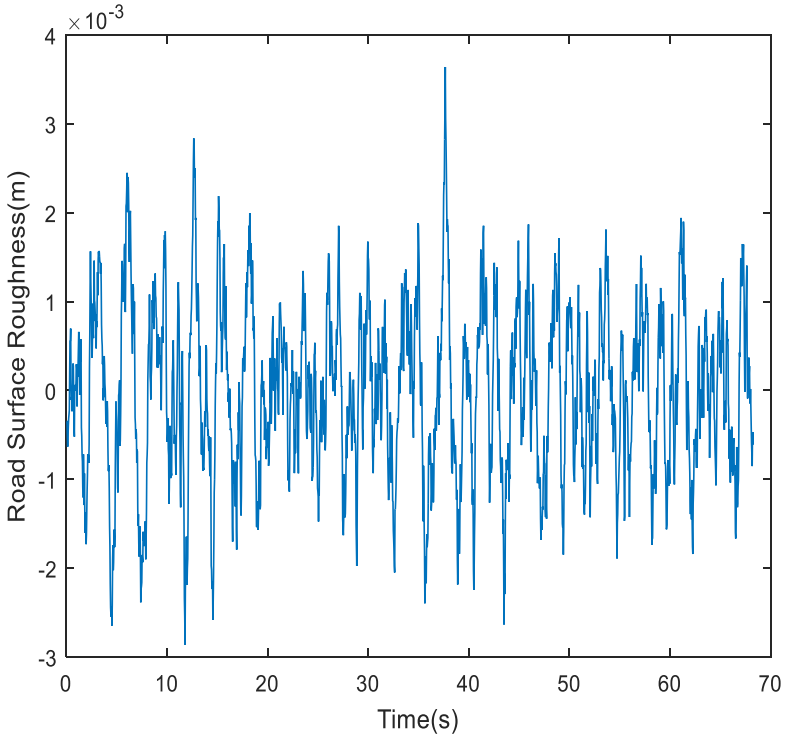

Figure 4: Road surface roughness with gravel road at 20Km/h vehicle speed

2.6 Vehicle Discomfort Parameter

When the human body is exposed to vibration, the comfort, working efficiency and, in some circumstances, health and safety of that body can be impaired. With increased exposure, tolerance of the human body to vibration is reduced and the feeling of tiredness is induced. The most important frequency region is 1Hz to 25Hz in which the human body is most sensitive to vibration in the vertical axis, with the 4Hz to 8Hz being most critical. A discomfort parameter can be defined as the weighted root-mean-square acceleration transmitted to the body in this frequency range. This is often measured in terms of the vertical rigid body acceleration of the vehicle body.

In order to assess passenger discomfort, it is necessary to determine the vertical acceleration response of the vehicle body over the frequency range of 1Hz to 25Hz. The appropriate weighting functions (human body sensitivity to vibration) are then applied to the response function.

Dynamic tire force measures the road holding ability. Within the range of highway speeds, some points along the road may be subjected to aggregate force depending on the roughness of the road surface and the speed of the vehicle. Dynamic tire forces are caused by interaction of a vehicle with road surface roughness. It is dependent on the vehicle design, vehicle speed and road surface profile. However, it is thought that the dynamic tire forces of heavy vehicles are significant causes of road damage, Mitchell and Gyenes (1989), Cebon (1988)

The damage caused at a particular point on a road by a vehicle depends on the forces generated by all the axles because all tires along one side of vehicle strike each point along the wheel path.

2.7 Simulink Block Diagram for Steady State Road Conditions

In order to investigate the dynamic response of vehicle under different vehicle speeds and road surface roughness profiles, Simulink block diagram (Figure 2) based on the dynamic equations of the model for steady state road roughness conditions is implemented.

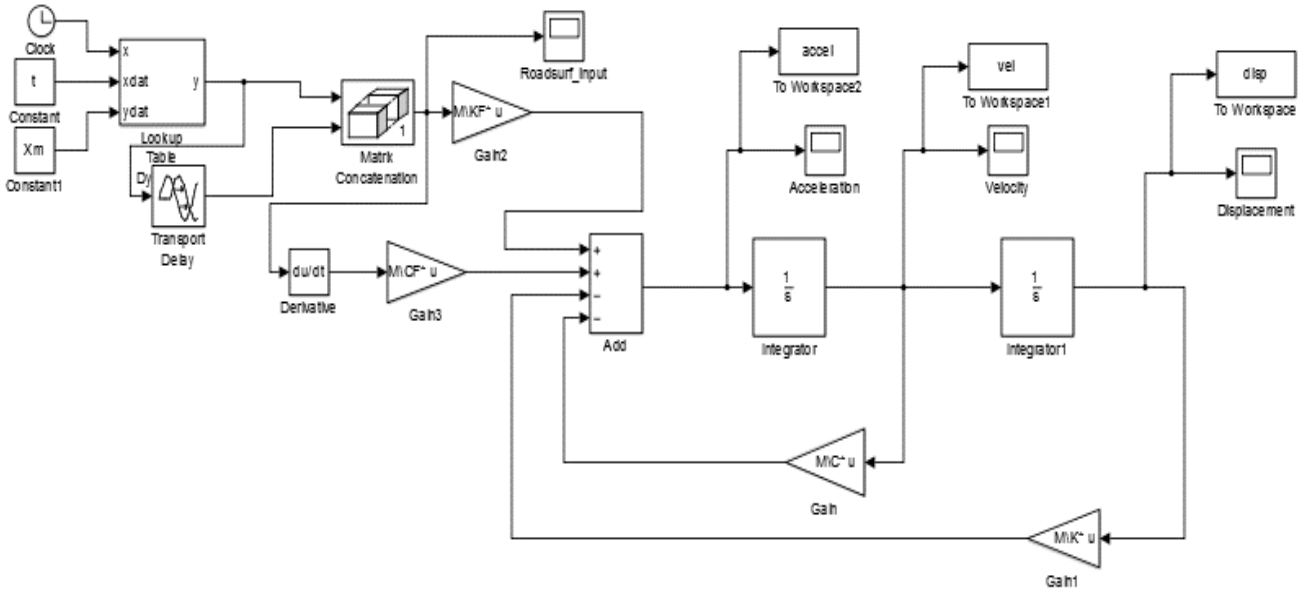

Figure 2: Simulink block diagram for road surface

The discomfort results obtained in the simulations will be compared with human discomfort zones as indicated in Table 4 (ISO 2631, 1997).

Table 4: Human Discomfort Zones (ISO 2631, 1997)

Discomfort Level	Remarks
Less than 0.315 m/s^2	Comfortable
0.315 to 0.630 m/s^2	A little uncomfortable
0.5 to 1 m/s^2	Fairly uncomfortable
0.8 to 1.6 m/s^2	Uncomfortable
1.25 to 2.5 m/s^2	Very uncomfortable
Greater than 2.5 m/s^2	Extremely uncomfortable

3. Results and Discussions

The rider's discomfort is based on the ride performance characteristics of vehicle suspension system can be assessed in terms of the vehicle body acceleration in relation to the discomfort, suspension travel and the dynamic tire force at different vehicle speeds from 20km/h to 80km/h. The range for comfort or discomfort according to ISO 2631 (1997) (Human comfort zone) are shown in the Table 4. From Table 4, daily exposure values of rider's body vibrations can be compared and assessed.

The Figures 5 and 6 show the relationship between rider discomfort at the lower and upper body of the human body respectively and change in vehicle speeds when traversing smooth, gravel and suburban roads.

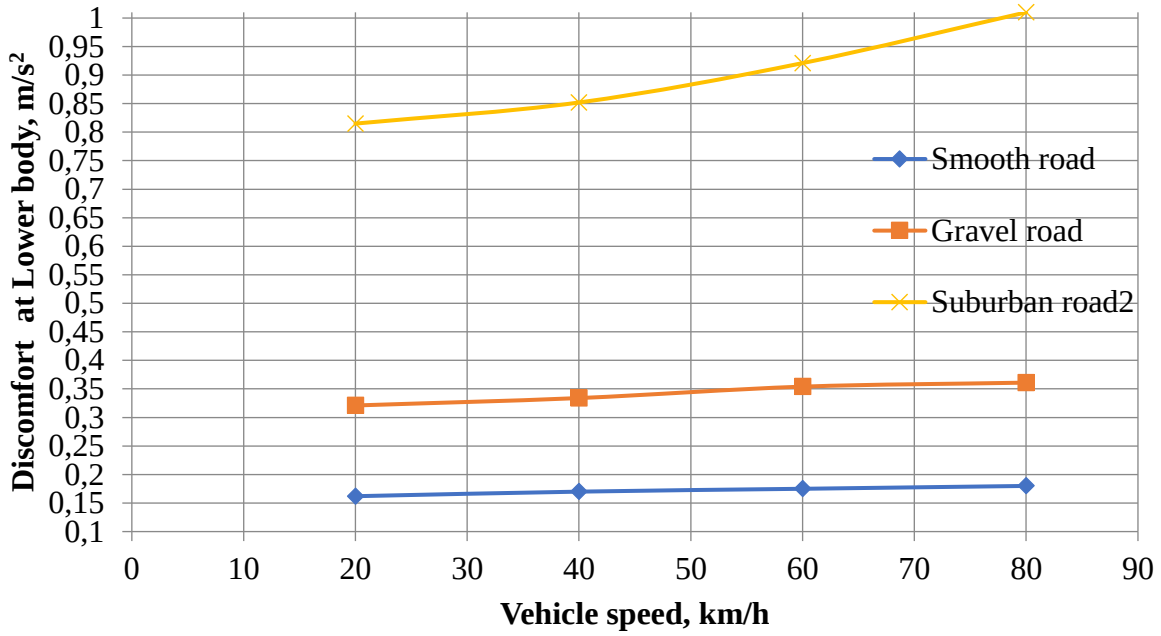

Figure 5: Discomfort at Lower body segment and different vehicle speeds over smooth, gravel and suburban roads

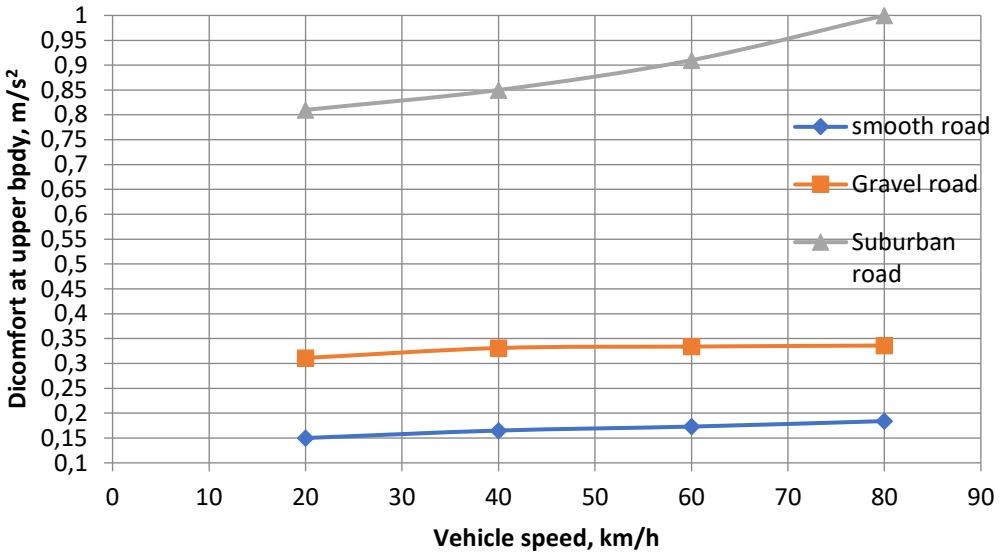

Figure 6: Discomforts at the Upper body segment and different vehicle speeds over smooth, gravel and suburban roads

Figures 5 and 6 showed that for each road surface conditions (smooth, gravel and suburban roads), the discomfort experienced at the lower and upper body segments increased as the vehicle speeds increased. According to Table 4 (ISO2631, 1997) the human tolerance zone of discomfort, rider of vehicle plying the suburban road experienced the highest discomfort compared to gravel and smooth roads while the discomfort experienced at the lower and upper body were lowest on smooth road.

3.1 Vehicle Suspensions Systems Under Steady State Road Conditions:

A parametric study was carried out to investigate the effects of various suspension parameters on the overall ride performance of the suspension system of the vehicle under steady state conditions at a vehicle speed of 20km/h. Each system parameter, shock absorber damping coefficient, tire stiffness, tire damping coefficient, etc was varied in turn while the other parameters were kept constant.

The result in Figure 7 is the plot of suspension stiffness of the vehicle suspension systems, and the corresponding discomfort at the lower and upper part of the human body. It shows that both the lower body and upper body segments did not experience discomfort in accordance with the values in Table 4 (ISO 2631, 1997).

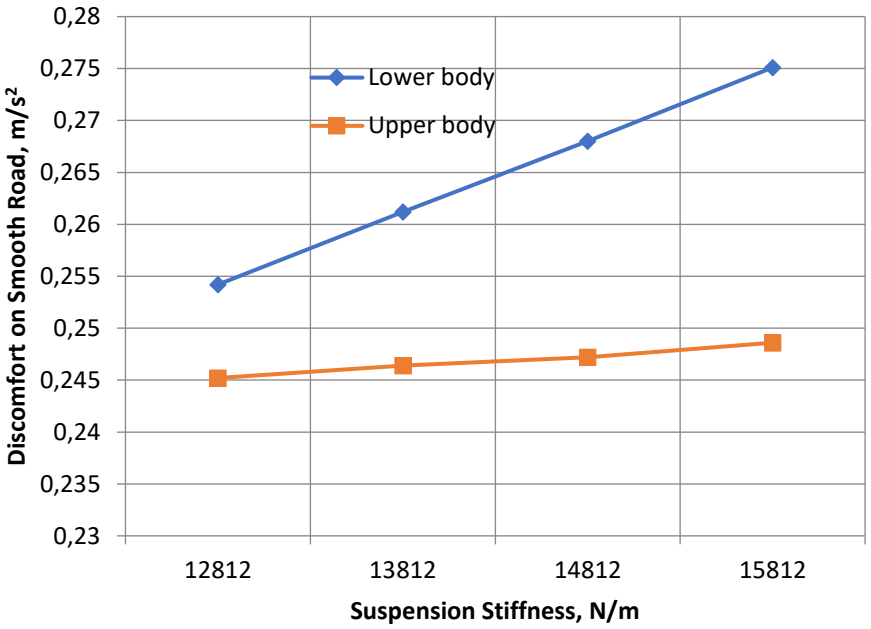

Figure 7: Suspension stiffness Discomfort at lower and upper body segments on smooth road

Figure 6 shows the plot of suspension stiffness with discomfort at the lower and upper segments of the human body. According to ISO 2631 (1997) the result shows that the lower body and upper body experienced discomfort as the vehicle traversed gravel road and also, as the speed increase

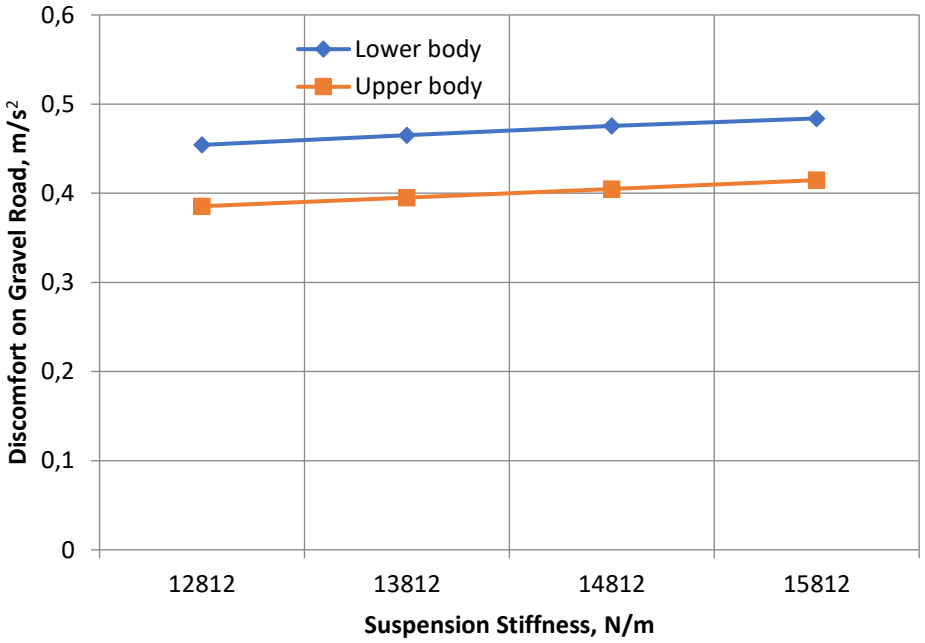

Figure 8: Suspension stiffness and discomfort at lower and upper body segments on gravel road

Figure 9 is the plot of suspension stiffness and discomfort at the lower and upper segments of the human body. According to ISO 2631 (1997), the result shows that the lower body and upper body segments experienced discomfort as the vehicle traversed suburban road and also, as the vehicle speed increase.

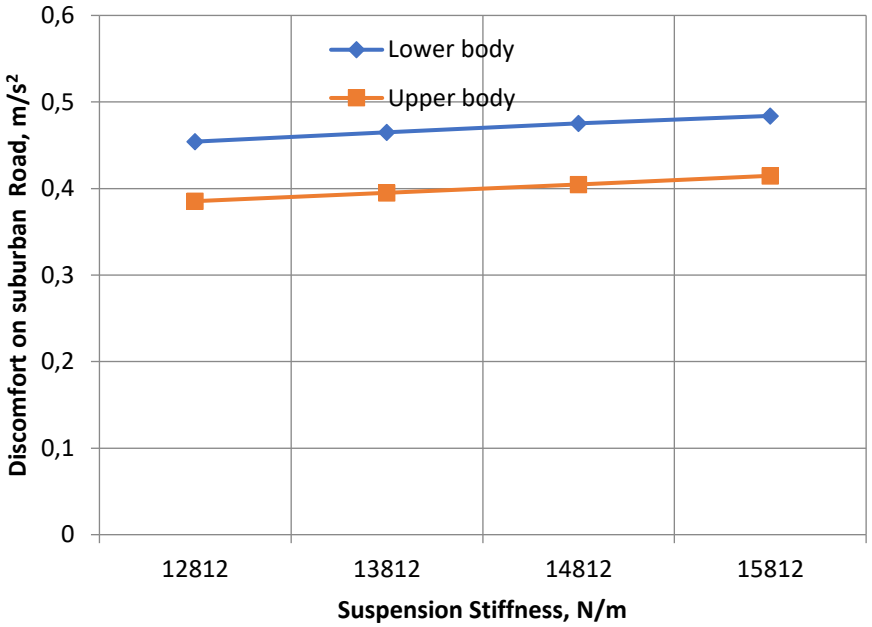

Figure 9: Discomfort at lower and upper body segments on suburban road with increase in Suspension stiffness

Figure 10 is the plot of discomfort and tire stiffness. It was observed that there was no discomfort when the vehicle traversed smooth road even when the tire stiffness is increased.

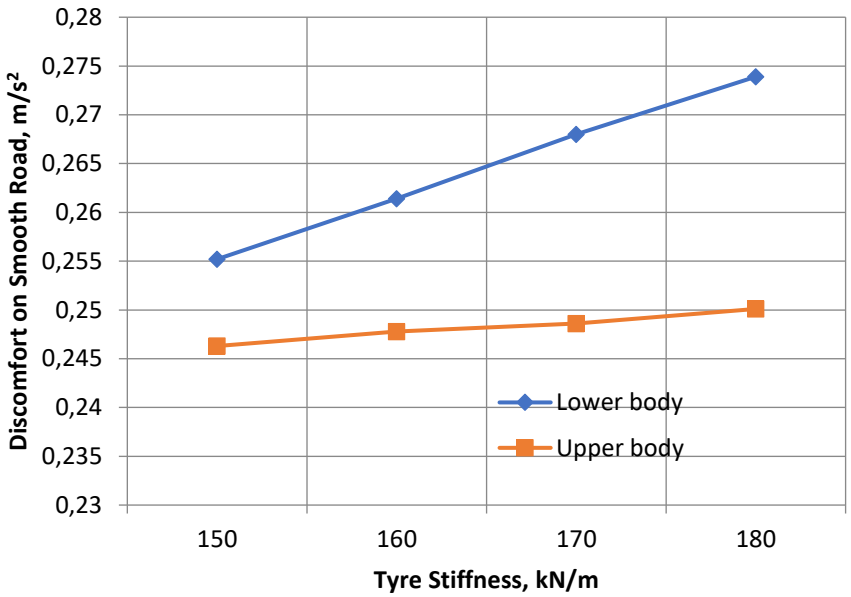

Figure 10: Tire stiffness and Discomfort at lower and upper bodies on smooth road

Figure 11 is the plot of tire stiffness and discomfort at the lower and upper segments of the human body. According to ISO 2631 (1997), the result shows that the lower body and upper body segments experienced discomfort as the vehicle traversed gravel road.

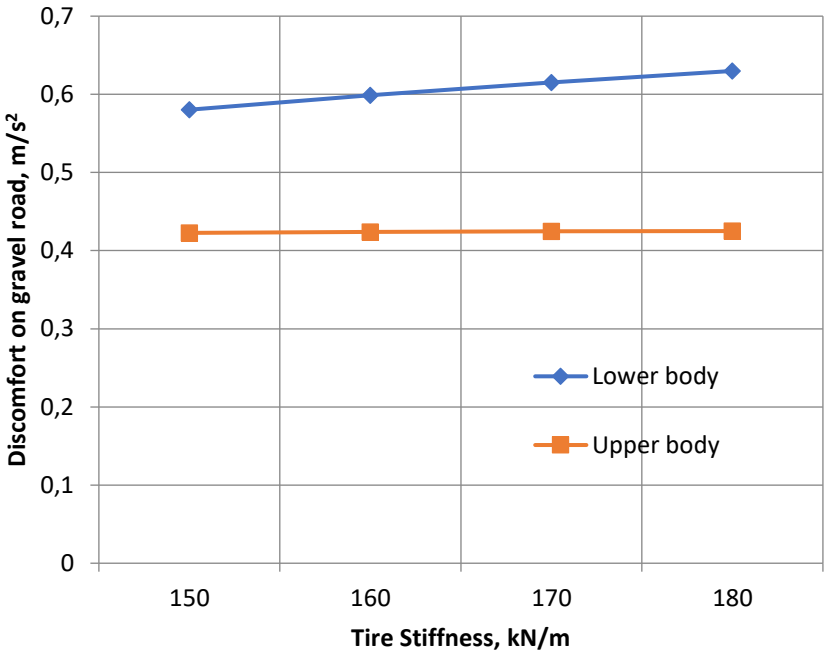

Figure 11: Discomfort with Tire stiffness at lower and upper bodies on gravel road

The same trends are recorded in Figure 12, in the plot of the vehicle tire stiffness and discomfort threshold. There is an increase in discomfort at the lower and upper body segments with increase in tire stiffness.

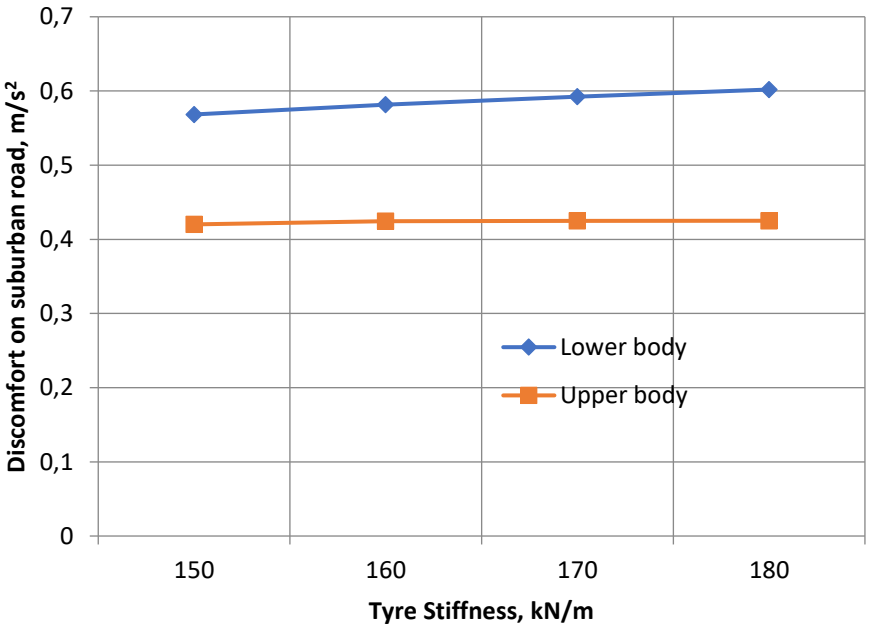

Figure 12: Tire stiffness and Discomfort at lower and upper body segments on suburban road

In Figure 13, the lower and upper body of the human body experienced comfort. The result agreed with the ISO2631.

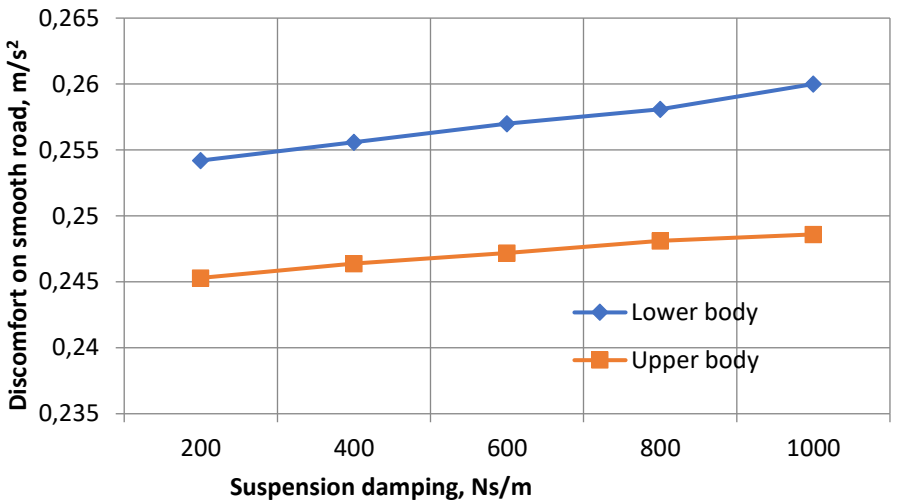

Figure 13: Suspension damping and Discomfort at the upper and lower body segments on smooth road

In Figure 14, the discomfort at lower and upper body road increased when the suspension damping was varied on gravel road.

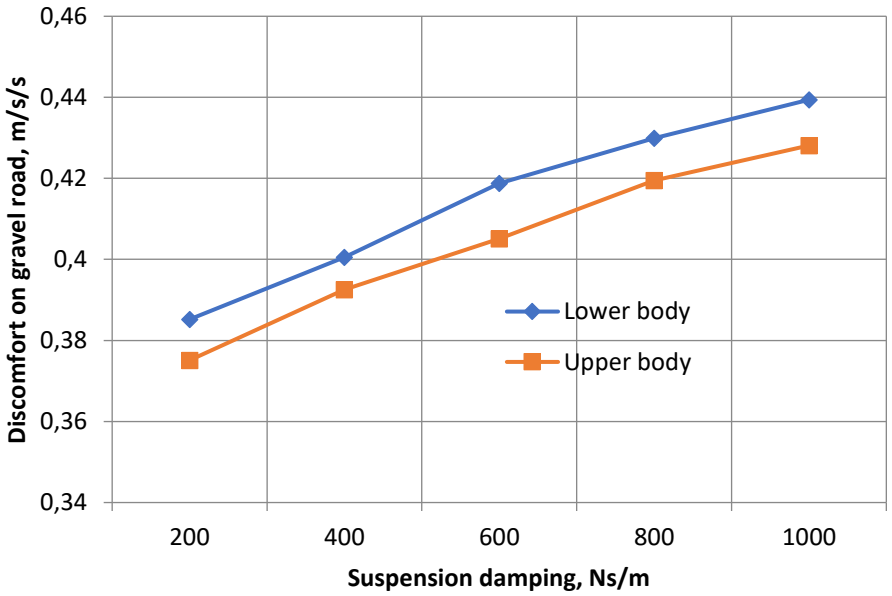

Figure 14: Suspension damping and discomfort at the upper and lower body segments on gravel road

In Figure 15, there is discomfort at lower and upper body segments on suburban road, and also, discomfort increased when the suspension damping was increased.

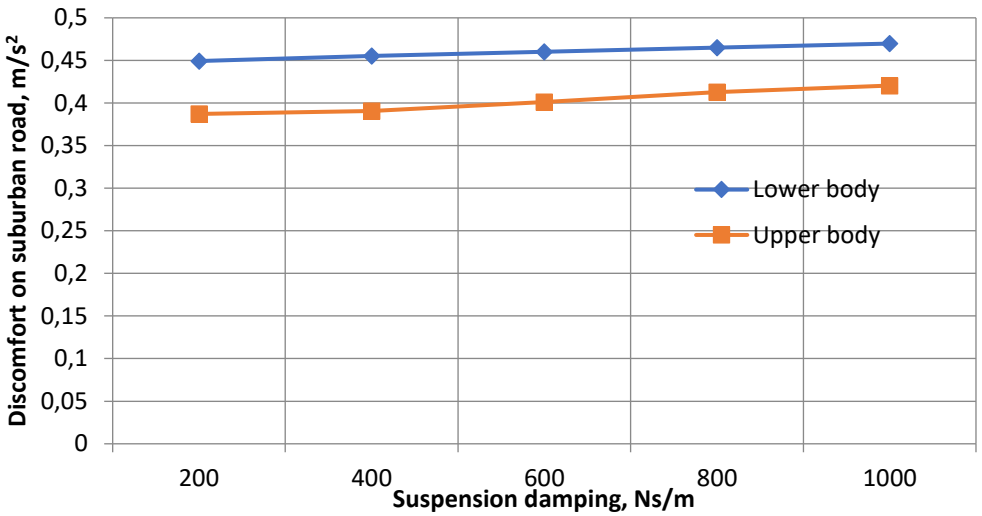

Figure 15: Suspension damping and Discomfort at the upper and lower body segments on suburban road

Figure 16 showed increase in suspension travel on the different roads as suspension stiffness is varied. Suburban road had the highest suspension travel due to higher roughness of the road.

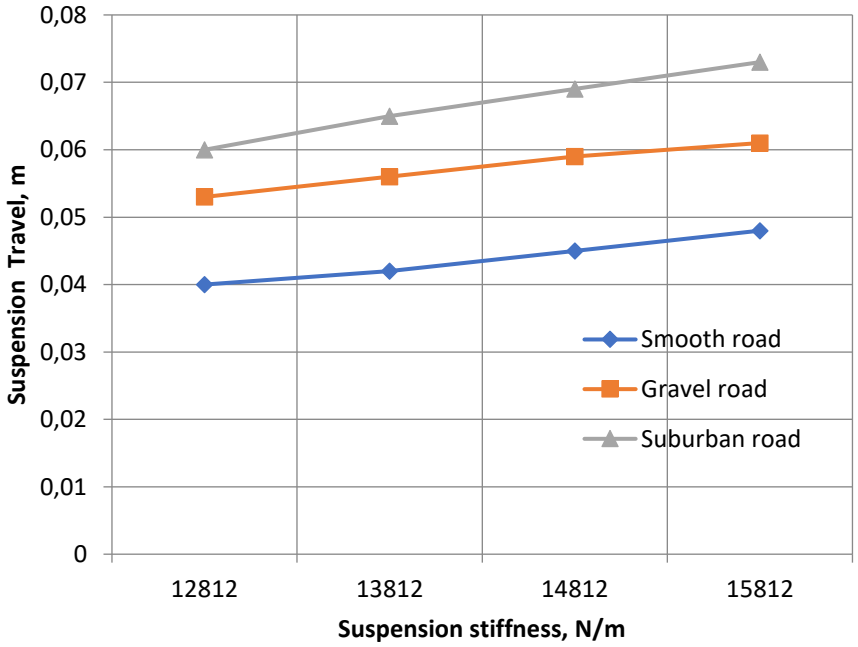

Figure 16: Suspension working space with suspension stiffness on smooth, gravel and suburban roads

Figure 17 showed increase in dynamic tire force on the different roads as suspension stiffness is increased. Suburban road had the highest dynamic tire force due to higher roughness of the road.

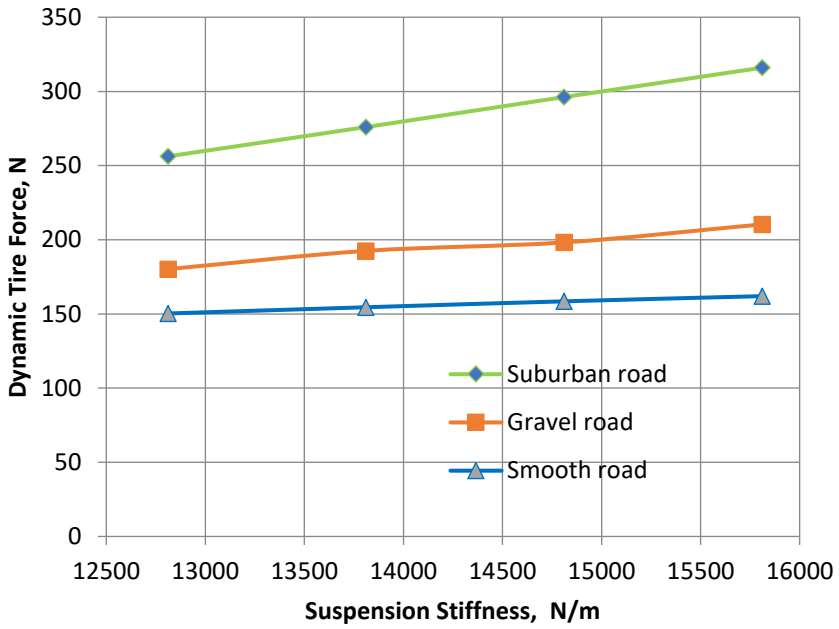

Figure 17: Dynamic Tire Force and Suspension stiffness on smooth, gravel and suburban roads

However, as the vehicle speed increased, the smooth road surface showed a small discomfort as the value corresponds to the recommended human tolerance zone of the ISO2631. Thus, the vehicle occupant experienced more comfort on the smooth road.

Figure 7 to Figure 15 show the discomforts experienced by the vehicle occupant at the lower and upper parts of the body on smooth, gravel and suburban roads when vehicle parameters such as suspension stiffness, tire stiffness and suspension damping were increased. According to ISO2631, discomfort increased considerably on the gravel and suburban roads with increase in vehicle parameters. However, there was little or no discomfort on the rider's bodies on smooth road as the values are within the comfort region (below 0.315m/s^2)

Figures 16 and 17 show the variations of dynamic tire force and suspension travel with suspension stiffness. The results show that the vehicle ride parameters increased considerably with increase in suspension stiffness on the different roads.

4. Conclusion

Parametric study of rider's comfort in a vehicle with semi-active suspension system under steady state conditions was carried out. MATLAB/SIMULINK software-based technique was used to obtain the performance of the vehicle suspension system, ride comfort of riders in relation to different road conditions using the semi-active suspension system were evaluated. The discomforts of the rider, suspension travel and dynamic tire force were assessed on the basis of ISO 2631 (1997). Semi-active vehicle suspension system reduced the discomfort experienced by the vehicle occupants on smooth.

The lower and the upper body segments of the vehicle rider experienced discomforts as the values are higher than the recommended ISO 2631 (1997) values. The results demonstrate that for each road surface, the discomfort grew as the vehicle speed increased. At each speed, the discomfort value over gravel and suburban roads surfaces were greater than smooth road (highway). The results show that the rider had exposure that exceed the recommended ISO 2631 (1997) human tolerance values of 0.315 m/s^2 and 2.5 m/s^2. Thus, the road roughness could be compensated through slowing

down of vehicle, thereby improving the ride quality on gravel and suburban roads thereby reduce the discomfort experienced.

References

Abbas. W., Abouelatta, O.B., El-Azab. M, Elsaidy. M and Megahed. A. A., (210) Optimization of biodynamic seated human model using generic algorithm, *SCRIP Journal of Engineering*, Vol. 2, pp710-719.

Abdel Hady, M.B.A and Crolla, D.A. (1989). Theoretical analysis of a active suspension performance using a four wheel vehicle model. Proceedings Institute of Mechanical Engineers, Vol. 203, Part D, PP. 125-135.

Ajayi, A. B., Ojogho, E., Adewusi, S. A., Ojolo, S. J., Campos, J. C. C., Siqueira, A. M. de O. (2023). Parametric Study of Rider's Comfort in a Vehicle with Semi-active Suspension System under Transient Road Conditions. *The Journal of Engineering and Exact Sciences*. **9(5).** 15287–01e. https://doi.org/10.18540/jcecvl9iss5pp15287-01e

Cebon, D., (1988). Theoretical road damage due to dynamic tyre force of heavy vehicles. Part1: dynamic analysis of vehicles and road surface; Part2: simulated damage caused by tandem-axle vehicle, *Proc. Institute of Mechanical Engrs*, Vol. 202, No C2, pp.103-117.

Davis, B.R and Thompson, A.G. (2001). Power spectral density of road profiles, *Vehicle System Dynamics*, Vol. 35, pp409-415.

Decky, M and Valuch, M., (2000). Road longitudinal unevenness as stationary ergodic process. Proceeding of International Conference, Durable and Safe Road Pavement, Poland, pp121-127.

Gohrle, C.A.; Schindler, A.; Wagner, A. and Sawodny, D. (2014). Design and vehicle implementation of preview active suspension controller, *IEEE Transactions on Control Systems Technology*, Vol.22, No.3, pp1135-1142.

Griffin, M.J. (1990). Evaluation of vibration with respect to human response. SAE paper, No.860047.

ISO2631 (1997). *Mechanical vibration and shock evaluation of human exposure to whole body vibration*- Part 1: General requirements, International Organization for Standardization.

Kim, M.H.; and Choi, S.B., (2016). Estimation of road surface height for preview system using ultrasonic sensor, Proceedings of the International Conference on Networking, Sensing and Control, pp. 1-4, IEEE.

Mitchell, C.G.B and Gyenes, L., (1989). Dynamic pavement loads measured for a velocity of truck suspensions, 2nd International Conference on heavy vehicle weights and dimensions, Kelowa, British Columbia.

Olatunbosun, O.A.; Dunn, J.W; (1991). A simulation model for passive suspension ride performance Optimization, Automotive Simulation' 91 (M. Heller) Springer Verlag pp131-142.

Raji, A, Venkatachalam., (2013). Frequency response of semi-independent automobile suspension system, *International of Engineering Research and Technology*, 2(10), pp 654-661.

Rouillard, V., Sek, M.A., Bruscella, B. (2001). Simulation of road surface profiles, *Journal of Transportation Engineering*, Vol. 127, pp247-253.

Sayer, M and Karamihasi, S., (1997). *The little book of profiling basic information about measuring and interpreting road profiles*. The University of Michigan, Transportation Research Institute.

Sharp, R.S and Hassan, S.A, (1986). Evaluation of passive automotive suspension systems with variable stiffness and damping parameters. *Vehicle System Dynamics*, 15(6), pp335-350.

Stoica, P, Moses, (1997). R.L., Introduction to spectral analysis. Upper Saddle River, N.J, Prentice Hall, pp. 5-9.

Sun, L. (2002). Simulating pavement surface roughness and IRI based on power spectral density. *Mathematics and Computers in Simulation*, No, 2, Vol. 61, pp77-89.

Thompson, A.G.; (1989). Optimum damping in a randomly excited non-linear suspension, Proceedings Institute of Mechanical Engineers, Vol. 184, Pt. 2A, No. 8, pp. 169-184